International Journal of Environmental Science and Technology
https://doi.org/10.1007/s13762-023-04767-2

ORIGINAL PAPER

Performance and characteristics of dynamic membranes for dairy wastewater treatment under anaerobic conditions

M. Paçal[1] · **N. Semerci**[1]

Received: 26 August 2022 / Revised: 30 December 2022 / Accepted: 6 January 2023

Abstract

The aim of this study was to treat dairy wastewater by using an anaerobic dynamic membrane bioreactor equipped with a 20-µm polyester mesh filter and at organic loading rate of 8.1 ± 1.5 kg COD/(m^3 day). The dynamic membrane was formed in 42 d, and the operation was continued for additional 50 days. In order to prevent membrane fouling and to ensure efficient cake layer formation, a wide range of cross flow velocity ranging from 5 m/h to 54 m/h was applied until a stable cake layer was formed. The chemical oxygen demand removal efficiency was 85 ± 9% in the dynamic membrane formation period (Day 0–42). In the stable operational period, the chemical oxygen demand removal improved by more than 10% owing to the well-developed Dynamic Membrane. Carbon, calcium, phosphorus, oxygen, and sulfur elements were detected in selected points of the dynamic membrane layer. Proteins and polysaccharides were detected in the dynamic membrane layer as organic compounds. The inorganic compounds in dynamic membrane layer were detected and found as 1.16% sodium, 1.50% magnesium, 0.76% potassium, 3.34% calcium, and 0.41% iron in mass concentration. The analysis results showed that organic and inorganic materials led to the formation of a strict/dense cake layer.

Keywords Anaerobic membrane bioreactor · Polyester mesh · Membrane filtration · Dynamic membrane components

Introduction

Huge number of dairy products are consumed around the world (Karadağ et al. 2015a). A large amount of water is consumed by dairy industries in order to manufacture dairy products. The wastewater, originating from dairy processing industry, includes high concentrations of chemical oxygen demand (COD), suspended solids (SS), carbon hydrates, proteins, lipids, and varying pH values (Britz et al. 2006; Joshiba et al. 2019). High organic content, a wide pH range and increased temperate are the factors that distinguish dairy wastewater because of requirement of special treatment to decrease or eliminate its negative impact on the environment (Slavov 2017). The dairy industry wastewater with high organic load cannot be removed easily (Joshiba et al. 2019). Activated sludge processes and anaerobic treatment are commonly applied for dairy wastewater treatment. High-energy requirements are one of the drawbacks of aerobic treatment processes (Bangsbo-Hansen 1985). Due to its high organic content and warm temperature, dairy wastewater is very suitable for anaerobic treatment (Elangovan and Sekar 2012).

Up-flow Anaerobic Sludge Blanket (UASB) is one of the applied reactors for this wastewater treatment under anaerobic conditions. Although UASB provides good removal performances, some difficulties are encountered during operation (Daud et al. 2018). Dairy wastewater includes a significant amount of lipids. The accumulation of these lipids causes undesired sludge floatation problems that result escape of biomass in UASB system (Karadağ et al. 2015b; Karthiyen and Kandasamy 2009). The integration of a membrane into bioreactor, a membrane coupled reactor, can decrease solid losses from the reactor. Anaerobic Membrane Bioreactor (AnMBR) can obtain very high solid–liquid separation efficiency and allows independent control of the sludge retention time (SRT) and hydraulic retention time (HRT). In addition, with the help of a membrane placed on the effluent line, the particulate organic substrate stays longer in the reactor

Editorial responsibility: Jing Chen.

✉ M. Paçal
mugepacal@gmail.com

[1] Environmental Engineering, Marmara University, Istanbul, Turkey

Published online: 21 January 2023

and can be hydrolyzed eventually and be degraded at long SRTs. On the other hand, there have been still obstacles in AnMBR applications, such as high cost of membrane modules, rapid membrane fouling during operation (Ersahin et al. 2012).

Membrane fouling presents an important disadvantage for conventional membrane filtration, whereas in the promising approach of Dynamic Membrane (DM) filtration, it is purposefully utilized for creating a low-cost, self-forming, reformed filtration surface (Ersahin et al. 2014; Alibardi et al. 2014; Zhang et al. 2014). DM layer consists of an underlying gel layer and cake layer. The gel layer forms through the attachment and deposition of the solutes and colloids on the support layer (e.g., nylon/dacron mesh) and strikes tightly to filter surface. Thus, allowing the use of cheap support material instead of conventional membranes enables an important cost reduction in the system. The large particles, which have attached loosely over gel layer, mostly constitute the cake layer. The cake layer can be removed physical cleaning methods, whereas the gel layer can hardly be scoured physically (Ersahin et al. 2012).

Both gel and cake layer are part of the DM layer. The important disadvantage of DM is membrane fouling, consisting of excessive cake layer. This makes reactor operation unstable and time-consuming owing to higher transmembrane pressure (TMP) and decrease in permeate flux (Mahat et al. 2018). DM layer should be controlled to prevent very thick layer that causes significant decrease in membrane permeability and increase in the TMP. There are studies about application of DM cleaning strategies (e.g., biogas sparging, cross flow velocity, physical cleaning) for effective DM layer control, complete DM layer detachment and reformation of DM to obtain longer and sustainable operation (Hu et al. 2018a).

UASB reactors are operated with ex situ DM modules, or in situ DM placed at the settling zone of UASB reactor to treat low strength wastewater (Siddiqui et al. 2021). There have been studies that the cake layer in submerged module was controlled by cross flow velocity (CFV) in DM-coupled UASB systems (Yang et al. 2020; Pacal et al. 2019). By applying CFV, the cake layer thickness (DM layer) can be controlled and high TMP and need for frequent membrane cleaning are eliminated (Alibardi et al. 2014). CFV simply creates a shear force that causes detachment of the loosely accumulated solids from the support material and slows down the cake layer formation. On the other hand, shear force is ineffective for smaller colloids that result blocking inside the pores of the filter (Wang et al. 2020). Besides, CFV also breaks up the sludge particles generating fine colloids and microbial cells that then form a denser cake layer on the membrane (Chang et al. 2002). Because higher CFV removes large particles, it enables the cake layer include small particles. These small particles lead to high cake compactness inside the cake layer (Ersahin et al. 2014) and induce higher TMP (Du et al. 2020).

Back-transport forces (Brownian diffusion, inertial lift and shear induced diffusion) occur depending on particle size in CFV system. These forces tend to raise with CFV and particle size, except Brownian diffusion. There is an inverse relationship between Brownian diffusion force and particle size (Wang et al. 2020). In most of the anaerobic dynamic membrane bioreactor (AnDMBR) studies, submerged/side-stream DM modules were integrated to continuous stirred-tank reactors (CSTRs) and DM formation was controlled with use of CFV. On the other hand, as mentioned before, application of CFV for the control of cake development on submerged DM modules in UASB reactors was tested in limited number of studies.

There are numbers of studies about dairy treatment by conventional membrane systems in literature (Dereli et al. 2019; Tan et al. 2021). Up to the present, the application of the anaerobic dynamic membrane bioreactor (DMBR) process for dairy wastewater treatment is limited to the previous study (Pacal et al. 2019). In the previous study, the average particle size distribution was 35 µm pore size in reactor. In addition, a cake layer, which formed on a nylon mesh with a pore size of 10 µm, exhibited a better treatment performance than that with a pore size of 70 µm. Considering results in the previous study, a support material having 20 µm pore size, which was close to 10 µm pore size, was selected for DM formation and filtration. In the previous study, the applied CFV was low and almost constant during synthetic wastewater treatment. In order to prolong filtration time under anaerobic condition, an alternative method (increase followed by decrease of CFV) in CFV application was used in this study.

Till this time, constant CFV has been mostly applied in DM-coupled UASB studies (Siddiqui et al. 2022; Pacal et al. 2019; Zhang et al. 2011) and the effect of CFV on DM formation has not been discussed conspicuously. On contrary to reported DM-coupled UASB studies, DM layer formation was controlled by way producing of the alternating CFV with internal recirculation (increase followed by decrease in CFV) in this study. The alternating CFV control procedure was applied for two aims. The first aim was to remove large particles causing sudden membrane fouling on support layer. The second aim was to enable the deposition of small particles on support layer in order to form a fertile DM layer, providing effective organic matter removal. The CFV was altered depending on change in flux and TMP as a result of solid accumulation.

The objective of this study was to assess the effectiveness of CFV in controlling the DM formation with an extended operation time on a submerged, tubular membrane module placed vertically in a UASB reactor and connected to the internal recirculation line. Thus, the anaerobic condition

could be prolonged without renewal of DM by operating system continuously with CFV. A detailed characterization of DM layer formed on the support layer, including inorganic and organic components, and morphology was determined and discussed in order to evaluate well-developed DM layer, enabling good treatment of dairy wastewater. The system was operated in Istanbul, Turkey for 92 days between 13 February and 15 May in 2019.

Materials and methods

Experimental setup

The experimental setup used in this study is presented in Fig. 1. AnDMBR system consisted of an UASB reactor that has a working volume of 3.8 L and a submerged tubular membrane module. The membrane module, which was made of polyester mesh (pore size = 20 µm, 13% of open area), was mounted in the cylindrical zone. The effective filtration area for the module was 0.012 m^2. A peristaltic pump (Watson Marlow 323) (pump 1) was used to feed substrate into the anaerobic reactor and to collect membrane-filtered effluent from the reactor. Another peristaltic pump (pump 2) was used both to recycle retentate from the membrane compartment to the reactor (internal recirculation) and to create CFV on the membrane surface. Pressure was measured by 0 ~ − 1 bar Mini Dial Vacuum Pressure Gauge Manometer (Aterna, Turkey) placed in the effluent line. The TMP was calculated as reported by Le Clech et al. (2003). The influent and effluent pHs were measured by probe daily (Hach, pH/ISE meter, United States).

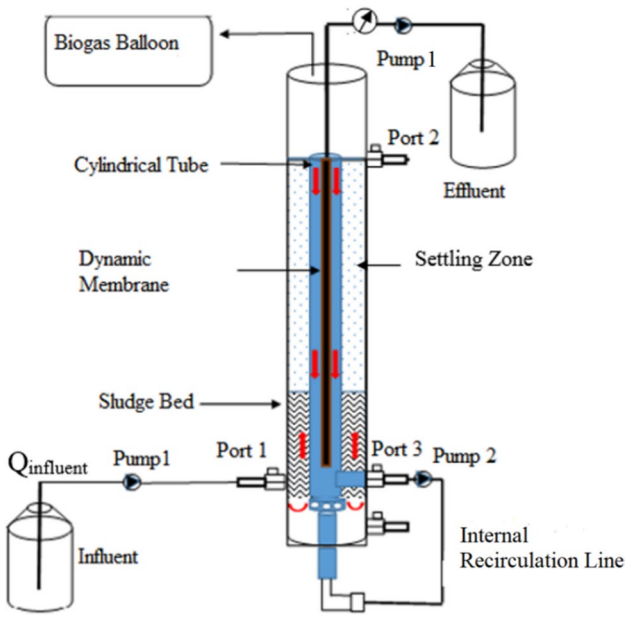

Fig. 1 Schematic view of the reactor system used in the study

Experimental procedure

A single laboratory-scale continuously fed UASB reactor was started-up with the gradual increase of COD loading rate using dairy wastewater before AnDMBR put into operation. AnDMBR operation lasted for 92 days. The influent characteristics of feed wastewater were given in Table 1. Organic loading rate (OLR) was kept at 8.1 ± 1.5 kg COD m^3/day. During the operation, the retentate flow was recycled into system by help of pump 2 (Port 3). During periods of increased TMP, the flow that cannot be drawn through the membrane was discharged through an overflow pipe (Port 2) located at the top of working volume of the reactor (Fig. 1). By this way, the water level in the reactor remained constant. Thus, a constant HRT of 27 ± 4 h was provided throughout the experimental period. Hence, retention time and membrane flux became independent from each other (Quek et al. 2017). The biogas was collected by biogas balloon. The gas escape from the effluent pipe was rarely seen.

As the permeability on membrane surface decreased, the membrane flux declined. The membrane flux changed between 12.1 and 1.1 L/m^2 h in DM formation phase. Through the end of the operation, flux decreased to 0.43 L/m^2 h. AnDMBR was operated at a constant temperature of 37 °C with the help of a heat jacket. The average pH values were 8.08 ± 0.52 in the effluent. Turbidity in the membrane effluent and the TMP were measured daily to monitor DM development. The CFV and backwashing were used to control the dynamic cake layer thickness on the surface of the polyester mesh. Backwash was done once in a day by reversing the direction of the effluent flow. It lasted for 15 min with a flowrate of 24.65 L/m^2 h. As seen in Fig. 1, CFV was created by taking retentate from the bottom of the cylindrical tube and returning it to the bottom of the reactor (internal recirculation) by using another peristaltic pump (Pump 2). The application method of CFV was to work with

Table 1 The characteristics of dairy wastewater

COD, mg/L	10,139 ± 766
Turbidity, NTU	10,125 ± 1792
SS, mg/L	4344 ± 660
pH	6.75
NH_4^+–N, mg/L	68
PO_4–P, mg/L	7.012
Ca^{+2}, mg/L	131
Protein, mg/L	3159
FOG, mg/L	1570
Carbohydrate, mg/L	5144

high CFV in order to reduce sudden increase in TMP caused by membrane fouling. Such that absolute membrane fouling can cause both important decline in flux, which hinder the system operation, and result sharp increase in TMP. If no significant change observed in decrease in flux, which resulted in a sharp increase in TMP, then the CFV was decreased to low values to stimulate the cake layer formation and eliminate unnecessary energy consumption. The CFV was selected according to reported studies (Hu et al. 2018a). The applied CFV was in a wide range of 5 m/h and 54.1 m/h. At the beginning of operation, CFV was 26.4 m/h. The CFV was raised up to 54.1 m/h to prevent membrane fouling and reduced to 5 m/h to avoid disrupting the cake layer during DM formation period. Depending on the flux, CFV was changed and kept at a constant value of 13 m/h from day 40 (toward the end of DM formation period) till the end of the whole operation.

Analytical methods

COD, SS, ammonium nitrogen (NH_4^+–N), orthophosphate as phosphorus (PO_4–P), fat, oil and grease (FOG) and volatile fatty acid (VFA) were analyzed according to APHA Standard Methods (APHA 2005). The average values of protein, carbon hydrate and calcium cation (Ca^{+2}) were calculated depending on nutritive value listed in semi-skimmed cow milk (Pınar, Turkey). The samples were taken from the membrane effluent and inside of the reactor (settling zone) with the help of port 2 to evaluate the effect of DM on treatment performance in terms of COD and SS removal. VFAs were analyzed using a gas chromatograph (Shimadzu GC-2014, Japan) equipped with a flame ionization detector (FID). The amount and the composition of biogas were measured daily by the water displacement method and gas chromatography (Shimadzu GC-2014ATF) equipped with a thermal conductivity detector (TCD), respectively. Turbidity measurements were carried out with Hach 2100 N turbidimeter. At the end of the operation, the entire cake layer deposited over the filter surface was removed prior to gel layer sampling. The cake layer was carefully scraped off by a plastic sheet and put into the cylindrical plastic tube. The sample was dried in 100 °C oven for analysis. The cake layer could be easily removed physically, but the gel layer was adhered to the support layer tightly and it was difficult to remove it physically. Thus, after cake layer on support material was taken, the support material, consisting of gel layer, was cut into small pieces for scanning electron microscopy (SEM) analysis. The virgin layer of support material, gel layer and cake layer were observed using the SEM. The samples were coated with aurum-platinum alloy for SEM analysis (Quorum, SC7620). The energy-dispersive X-ray (EDX) system (Zeiss, Evo Ma 10) was applied to determine the major elements of the DM layer. Particle size distribution (PSD) of SS both in the reactor and in the cake layer was measured by a Mastersizer 2000 (Malvern Instruments, Hydro 2000 MU), an instrument that uses a laser diffraction technique to measure the sizes of particles with a detection range of 0.1–2000 µm. ICP-MS was conducted with an Apilent 7700 to analyze inorganic elements on DM. An FTIR spectrometer (Jasco FT/IR-4700, Japon) was employed to characterize the major functional groups of DMs. The spectrum was calculated over the wave number ranging from 4000 to 400 cm^{-1}.

Seed sludge and raw wastewater characteristics

The reactor was inoculated with anaerobic granular sludge produced under mesophilic conditions from an expanded granular sludge bed (EGSB) reactor at the cartoon industrial wastewater treatment plant, İstanbul, Turkey. The initial concentration of the granular sludge was 50 g/L. Diluted milk, which had almost the same content as the dairy industry wastewater, was used as wastewater. Thus, dairy wastewater was prepared daily by dissolving 10 g of semi-skimmed cow milk (Pınar, Turkey) in 1 L of tap water. The characteristics of dairy wastewater are presented in Table 1.

HRT, the flux and permeation resistance measurement

The HRT was calculated by dividing the reactor volume by influent flow rate (Q_{influent}) (Eq. (1)

$$\text{HRT} = \frac{V}{Q_{\text{influent}}} \tag{1}$$

The membrane flux J (L/m^2h) was determined by weight of treated water and calculated according to Eq. (2).

$$J = \frac{L}{A \times t} \tag{2}$$

L denotes the volume of permeate liquid per unit membrane area (A), and t refers to filtration time. Total filtration resistance is a function of TMP, the flux, and viscosity of the water. The filtration resistance at each step was calculated using Eq. (3):

$$R = \frac{\text{TMP}}{\mu \times J} \tag{3}$$

where R is the permeation resistance, TMP is the transmembrane pressure drop (mbar), μ is the viscosity of the filtrate (0.697×10^{-3} Ns/m^2 at 37 °C), and J is the membrane flux of the AnDMBR module.

Results and discussion

Effect of CFV on DM formation

The CFV was changed three times to keep the cake layer in a certain thickness during the formation period by the combination of increasing and decreasing of its value within a wide range. The initial flux was approximately 11 L/(m^2 h) (Fig. 2a). As soon as the AnDMBR was taken into operation, particles retained on the support layer which was observed through a sharp decrease in flux on day 2. The permeation drag force that is induced by the membrane flux uses this force on the particle by way of the water permeating through the membrane (Ramon and Hoek 2012), thereby resulting in both adsorption and deposition of solids on the surface of support layer. In addition to this, the initial TMP was 28 mbar and on day 2, TMP increased by 2.42 times (68 mbar) of its initial value (Fig. 2a). Although internal recirculation was in operation from the beginning of the operation, the CFV was not enough to sweep away this accumulated particle on support layer. The CFV was almost same between days 1 and 3. Due to the fast increase in TMP on day 3 (311 mbar), the CFV was increased gradually and set to 54 m/h on day 5. As a result, higher shear forces created by CFV caused back-transport of loosely accumulated solids on the support material and slowed the membrane fouling that TMP decreased to 77 mbar on day 5. The particles could not accumulate effectively on support material (day 1–4) that the membrane flux restored on day 5 with high CFV. In addition, more particles flowed into cylindrical tube by help of higher CFV (day 2–5), created by higher internal recirculation. These particles were exposed to higher CFV such that this could cause forming of smaller particles as a result of breaking of larger particles by high CFV (Wang et al. 2020; Chang et al. 2002).

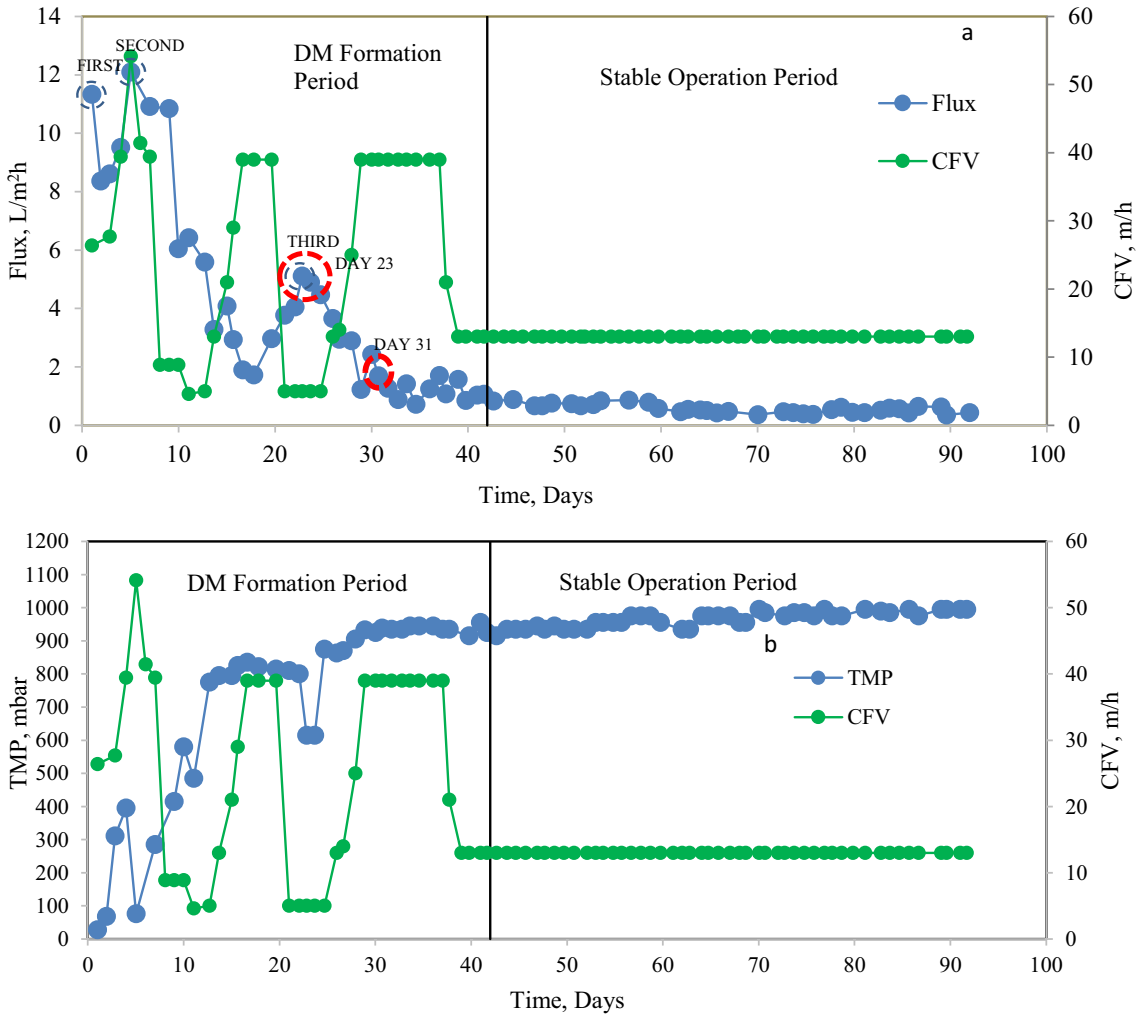

Fig. 2 Flux and CFV (**a**) and TMP and CFV (**b**) determined during the AnDMBR operation

As the permeability was restored on day 5 (Fig. 2a), the CFV lowered gradually in the following days to form cake layer and cause less energy consumption during operation. The CFV decreased gradually to 5 m/h (day 11) from 54 m/h (day 5) and remained at 5 m/h for 2 days. As seen in Fig. 2a, the decrease in CFV resulted increase in particle deposition on support layer in the following days. Between day 5 and day 18, the membrane flux gradually declined, which corresponded to a flux reduction of 8%/d. The second decline in flux was slower than the first. The first reason of this was that higher CFV prevented deposition of larger particles on support layer. The second reason was the increase in CFV (day2–5) could result in formation of particles, which was smaller than pore size of nylon mesh, and this could slow down deposition of particles on support layer.

The decline trend (between day 5 and day 18) in flux was close to Sun et al. (2018) who reported sharp decrease in flux as a result of initial sludge deposition on support layer during DM formation. In this study, the deposition of particles was controlled by shear force to prevent sudden membrane fouling, including excessive cake layer formation.

Both the increase and decrease (from day 5 to day 13) in CFV prolonged deposition of particles on support layer and provided effective cake layer formation on support layer such that sharp decline in flux happened (day 18), and turbidity decreased to (46 NTU) 4.6% of its initial value. In addition to these, a rapid rise in TMP was observed after day 5 and it reached 775 mbar on day 13.

In order to control this increase in TMP, the CFV increased gradually from 5 m/h (day 13) to 39 m/h (day 17) and was kept at a high level for more 3 days. The reason for the increase of less CFV (39 m/h) than the first (54 m/h) was not to disrupt the layer formed on the support material. After day 18, an increase in flux and turbidity began. A gradual recovery of flux in the following days (from 1.71 L/m^{2}h on day 18 to 5.10 L/m^{2}h on day 23) was observed because of this increase in CFV in previous days. In addition to this, the TMP was sharply decreased from 800 mbar (on day 22) to 615 mbar (day 23). The TMP remained at this value for one more day. The periods of increased CFV resulted in turbidity spikes in the effluent after day 18 (Fig. 3), owing to broken of solid depositions formed on the support layer. Thus, in order not to disturb DM layer, the CFV was decreased after day 20, and the reactor continued to operate at a lower CFV of 5 m/h for 5 days.

The third decline in membrane flux began after day 23. The TMP increased sharply to 875 mbar on day 25. In order to control this increase, the CFV was gradually increased (from 5 m/h on day 25 to 39 m/h on day 29). The CFV was maintained at 39 m/h for 9 day. However, the flux decreased from day 23 to day 31 gradually, and TMP reached 938 mbar. After day 31, no considerable increase in flux was observed. A gradual decline was observed in

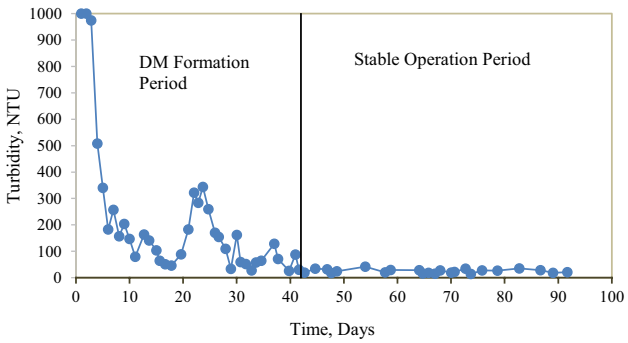

Fig. 3 Turbidity during the AnDMBR operation

flux (from day 23 to day 31), which took a longer time than the previous decline (from day 5 to day 18). This could be explained by working in lower CFV, which was in the range of 5 m/h and 39 m/h (from day 23 to day 31) (Fig. 2a). After day 31, the membrane flux continued to decrease slowly, and no considerable change in effluent turbidity and TMP occurred, as well. This showed that the CFV lost its effect on membrane permeability. As mentioned by Alibardi et al. (2014), the consolidated cake layer decreases effectiveness of the CFV. The CFV was decreased from 39 m/h (day 37) to 13 m/h (day 39). The CFV was maintained at this value until the end of operational period. The membrane flux continued to decrease at a very slow rate. From day 31 to day 42, it could be inferred that transport of particles to membrane by flux decreased slowly until it was almost balanced with back-diffusion of particles (from DM to feed solution) at steady state (Forero et al. 2013). The membrane flux declined to 1 L/(m^2 h) on day 42 and continued to decrease very slowly. Moreover, a slight increase in TMP to 925 mbar occurred on day 42 (Fig. 2b). The applied CFV procedure prolonged DM formation and operation under anaerobic condition. Thus, filtration time lasted longer than the previous study without any need for physical cleaning.

In the DM application, cake layer formation is a significant factor that determines the flux. Thus, other factors such as biological operational conditions, temperature, and substrate type have less of an effect on the flux (Ersahin et al. 2012; Jeison and Van Lier 2007). It is very important to control the cake layer thickness to obtain efficient solid retention and stable filtration with DM technology. This is because cake layer formation offers solid retention inside the bioreactor but also induces an increase in the filtration pressure (Ersahin et al. 2012). Hu et al. (2018b) studied with two UASB reactors to compare the effect of sludge recycle on DM formation. They found that sludge recycle, inducing higher CFV, was unnecessary for DM (75 μm) formation. However, in this study, CFV was applied in wide range by using internal recirculation and this was found to be beneficial for cake layer formation.

Moreover, the applied CFV was less than 1.8 m/h in reported UASB integrated submerged DM studies with a pore size of 65 µm (Zhang et al. 2011) and 75 µm (Yang et al. 2020). One of the reasons of this lower CFV application could be due to reactor characteristics. Such that the membrane was integrated into top of UASB reactor in these studies, whereas the membrane was in narrow membrane compartment in this study. The narrow cross section of the membrane compartment caused high CFV in this study (Fig. 2).

However, Alibardi et al. (2014) performed a low CFV of 1 m/h for initial cake layer formation and then higher CFV (5–360 m/h) to control cake layer thickness and membrane permeability in CSTR integrated DM study with a large pore size of 200 µm. Moreover, there have reported CSTR integrated DM studies where constant CFV was applied (10 m/h–35 m/h) (Siddiqui et al. 2021). In this study, the CFV was operated within a wide range (up to 54 m/h) during DM formation stage and then the operation was continued with constant CFV (13 m/h).

The CFV applied in this study was consistent with most AnDMBR studies (Siddiqui et al. 2022, 2021). However, in contrast to DM-coupled UASB studies, the CFV was applied in a wide range during the DM formation stage to control both cake layer thickness and membrane permeability. As mentioned by Chang et al. (2002), the increase in CFV caused the formation of small particles which resulted in a denser cake layer formation. The decrease in CFV enabled effective accumulation of solids over a support layer, resulting distinctively decrease in turbidity in the membrane effluent. In addition to this, the recycle, which induced CFV, provided more sludge in suspended in the reactor. Thus, as recycle was increased, more particles overflowed into membrane compartment (Fig. 1). This improved solid contact with membrane surface in this study.

Moreover, DM forms faster on smaller pore size support material and thus a high pollutant removal can be obtained by a small pore size (Li et al. 2017). In contrast to the reported study by Hu et al. (2018b), by studying with wide range CFV, a well-developed DM was obtained with a smaller pore size that resulted in high pollutant removal in this study. All these results showed that operation mode (such as pore size of support layer) seemed to be important factor for CFV application procedure.

DM formation and the stable operation phase

As the cake layer was formed on the support layer, the filtrated water become cleaner. The turbidity decreased to 31 NTU on day 42 (Fig. 3). This was called the DM formation period. The permeate flux decreased from 12.1 L/(m^2 h) to 1.1 L/(m^2 h) at the end of this period. In the following days, the turbidity became almost stable (25 ± 6 NTU), which indicated that the DM formed (Li et al. 2017). This value is consistent with Ersahin et al. (2017), who reported stable turbidity with a value of 30 ± 2 NTU in effluent. After DM formation (day 42), the membrane flux continued to decrease more slowly than in the previous period. The membrane flux decreased to 0.5 L/(m^2 h) on operation day 62. The membrane flux continued at this average value [0.50 ± 0.08 L/(m^2 h)] from that day (day 62) until the end of the operational period. This period was concluded after 50 d and ended with a membrane flux of 0.43 L/(m^2 h). This period was called the stable operational period (Fig. 2a).

In DM application, cake layer permeability is the most significant factor that manages the flux.

The change in flux during the study confirmed the observations reported by Tang et al. (2017) and Sun et al. (2018). Satyawali and Balakrishnan (2008) obtained stable fluxes between 0.8 L/m^2 h and 0.9 L/m^2 h operating a DMBR equipped with a submerged membrane module characterized by a nominal pore size (30 µm). A low flux of 0.1 L/m^2 h was reported by Kooijman et al. (2017) during the operation of a laboratory-scale AnDMBR treating waste activated sludge. Li et al. (2017) reported that DMs formed on a larger pore size mesh usually possessed a somewhat greater flux, and the selected pore size influenced the filtration flux. The pore size in this study was parallel with these reported pore sizes.

Membrane resistance

As mentioned in effect of CFV on DM Formation section, the TMP reached 925 mbar on day 42 owing to the decrease in membrane permeability and was approximately 964 ± 23 mbar in the stable operational period (Fig. 2b). The TMP progress in this study validates the TMP profile reported by Ersahin et al. (2017). However, the TMP values in this study were higher than the values reported in some previous studies, which were in the range of 4.9 mbar to 800 mbar. (Hu et al. 2018a). This result can be explained by operation modes. The mesh with smaller pore sizes retains more solids that this decreases membrane permeability. The mesh with small pore size causes high TMP in many cases (Siddiqui et al. 2021). In addition to this, Yang et al. (2020) reported that decrease in HRT resulted increase in TMP. In this study, the pore size and applied HRT was lower than some DM studies (Hu et al. 2018a). It should be added that there was reported anaerobic DMBR study, in which TMP value was 2000 mbar (Ersahin et al. 2012). Moreover, TMP value in this study was higher than the previous study. As mentioned by Ersahin et al. (2017), high TMP was likely caused by thick DM layer. Hu et al. 2018b reported that TMP increased with the increase in OLR because of accumulation of more fine particles and colloids on support layer. Thus, in addition to the reasons mentioned above, the applied

higher loading rate in this study could result in high TMP by accumulation of more solids on support layer. The typical operating pressure was reported to be 1000–4000 mbar for MF and 2000–7000 mbar for UF. The studied DM pressure was lower than those reported for conventional membranes. This showed the advantage of DM operation owing to its low energy cost.

The DM formation time in this study was higher than in some previous studies (Ersahin et al. 2014; Alibardi et al. 2016). This could have been due to the low contact of solids with the support material. As mentioned by Ersahin et al. (2014), the time required to form an effective DM layer could be related to the morphology and concentration of the sludge, characteristics of the support material, feed type, and operational conditions. Moreover, membrane resistance is an important indicator for effective cake layer formation. As particles were adsorbed and deposited on the support layer, membrane resistance began to increase in the DM formation period and continued to increase in the stable operational period. The membrane resistance reached 4.71×10^{10} m^{-1} and 1.16×10^{11} m^{-1} in the DM formation and stable operational periods, respectively (Fig. 4). The change in CFV caused fluctuations in the TMP and flux until it lost its efficiency in DM operation. After the DM formed, the membrane resistance improved with a very slow decrease in flux and increase in TMP as a result of the solids accumulation on the DM layer. As mentioned by Sun et al. (2018), the DM filtration resistance was affected by the deposited solid mass. Thus, the slight increase trend in the stable stage was explained by continuity of accumulation of solids on DM. Membrane resistance is governed by the membrane pore size and membrane surface porosity (Judd 2006). As the pore size increases, the membrane resistance decreases. Moreover, biomass characteristics (PSD) and operational conditions (HRT) are other important factors for cake resistance (Lin et al. 2013). These factors are inversely proportional to cake resistance. Sun et al. (2018) calculated the membrane resistance as 1.73×10^{10} m^{-1} and 6.68×10^{10} m^{-1} at the end of DM formation and the end of sustainable flux (30 µm) coupled with CSTR, respectively. The membrane resistance in this study was slightly higher than the values that found by those researchers. This could be due to the pore size of the studied support material. In addition, in this study, the membrane resistance in the end of the stable operating period was consistent with Tang et al. (2017), who reported DM resistance as 1.3×10^{11} m^{-1}. The reported Microfiltration/Ultrafiltration (MF/UF) membrane resistance was in the range of 10^{11}–10^{14} m^{-1} (Lin et al. 2009). Thus, as mentioned by Sun et al. (2018), this lower membrane resistance in the DM shows superiority over other conventional filtration units in terms of the high-energy savings and filterability of the AnDMBR. As a result, it is possible to achieve high efficiency of the DM in wastewater treatment applications, which provides both high organic matter removal and low operating costs.

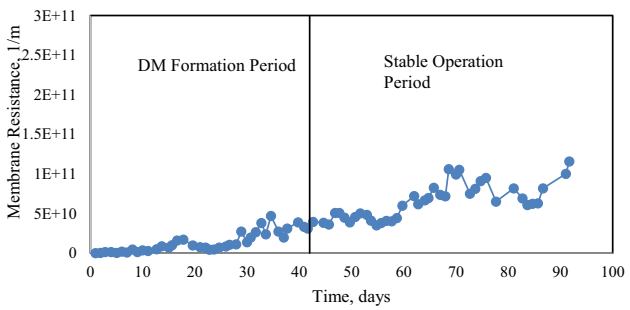

Fig. 4 Membrane resistance during the AnDMBR operation

System treatment performance

The COD concentration in both the reactor (settling part of the reactor) and membrane effluent during the operational period are presented in Fig. 5a and Fig. 5b, respectively. In the DM formation period, the COD concentration was approximately 818 mg/L in the membrane effluent and the COD removal efficiency was 85 ± 9%. From operation days 42 to 92, the COD removal was 99.0 ± 0.6% (Fig. 5b). The average COD concentration in the reactor was 1467 ± 350 mg/L (Fig. 5a), whereas the average COD concentration in the membrane effluent was 127 ± 31 mg/L during the stable operation phase (Fig. 5b). This showed that the membrane module improved COD removal in the effluent. The cake layer formed on the support layer caused both biodegradation in the DM layer and solid retention. An effective combination of solid retention and biomass activity in the DM layer was responsible for the higher COD removal in this system. Organic matter, such as polysaccharides, proteins, and microorganisms (colloidal matter), accumulated on the support layer, and a biofilm formed. The biofilm provided both solid–liquid separation and organic matter removal; thus, it improved the COD removal efficiency. A greater amount of organic matter was removed with a COD loading rate of 8.1 ± 1.5 kg/(m^3 day) in this study. Elangovan and Sekar (2012) reported that a UASB reactor could achieve 70–90% COD removal with 2–15 kg COD/(m^3 day) and an HRT of 8–50 h during dairy effluent treatment. Thus, in this study, COD reduction of dairy processing wastewater was improved by the help of an inexpensive DM module. The obtained COD removal efficiency in this study was higher than this reported in UASB study.

Couras et al. (2015) obtained 81 ± 5% and 85 ± 6% COD removal with COD loading rates of 3 kg COD/m^3 and 10 kg COD/m^3, respectively, with two UASB reactors treating diluted semi-skimmed milk. However, this study showed that a higher COD removal could be obtained by integrating

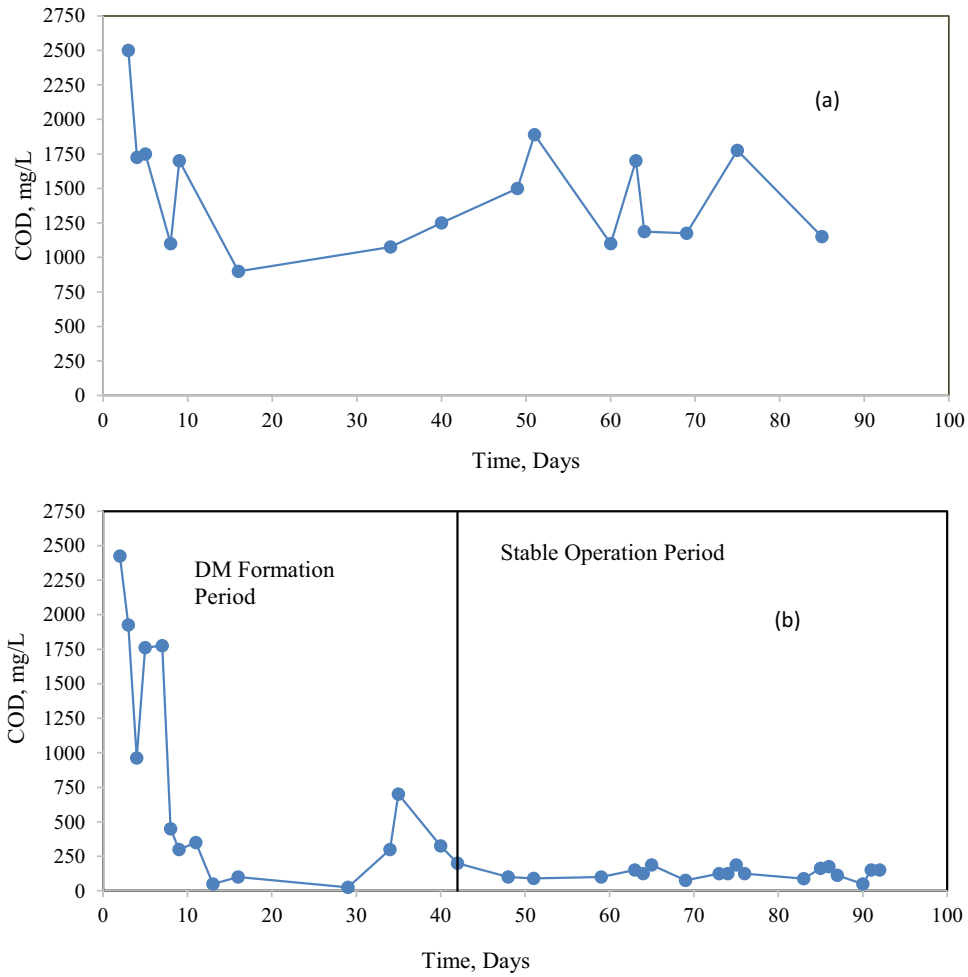

Fig. 5 COD in the settling zone of the reactor (**a**) and COD in membrane effluent (**b**) during the AnDMBR operation

a simple nylon mesh into a UASB instead of working with more reactors.

In a study, synthetic dairy wastewater was treated with a COD removal rate of 92 ± 3% with OLRs of 1 kg COD/m^3 (HRT: 72 h) and a COD removal rate of 91 ± 2% with OLRs of 2.96 kg COD/m^3 (HRT: 24 h), respectively, by a Hybrid Anaerobic Baffled Reactor (AnBR) with total volume of 25 L, including five compartments (Giordani et al. 2021). In comparison with the treatment performance of reported dairy wastewater study, high-strength wastewater (dairy wastewater) could be treated by only a reactor equipped with a low-cost membrane. This showed the superiority of AnDMBRs over other reactors in terms of their high treatment performance and low operational cost.

In this study, COD removal efficiency was higher than the reported values for wastewater treatment by DM-coupled UASB systems. Quek et al. (2017) obtained COD removal efficiencies of 71% (HRT: 6 h) and 64% (HRT: 3 h) with OLRs of 1.5 kg COD/(m^3 day) and 3.0 kg COD/(m^3 day) during AnDMBR operation, respectively. Hu et al.(2018b) reported a COD removal efficiency in the range of 72% and 92% (HRT:8 h) during municipal wastewater treatment with COD loading rates of 0.88, 1.55, and 3.01 kg COD/(m^3 day). A COD removal rate of 74.4% (HRT: 8 h), 77.3% (HRT: 4 h), 70.6% (HRT: 2 h) and < 60.4% (HRT:1 h) were obtained by Yang et al. (2020) during domestic wastewater treatment with a COD loading rate of 0.82–6.80 kg COD/(m^3 day).

Studies have found that DM-coupled CSTR systems obtain COD removal efficiencies mostly higher than 89% (Siddiqui et al. 2021). Until now, COD removal efficiency has exhibited limited performance in DM-coupled UASB systems. In this study, high COD removal exceeding 99% was obtained by a DM-coupled UASB system. This was because internal recycling provided SS and increased contact between the solids and support material. This caused efficient cake layer formation. A well-developed DM caused high organic matter removal in the DM-coupled UASB system. Moreover, COD in the membrane effluent met the industrial wastewater effluent discharge regulations in Turkey.

In addition to what is mentioned above, it should be emphasized that longer HRTs result in higher COD removal rates (Pacal et al. 2019). Moreover, disadvantage of studying

with high OLR is accumulation of VFA. Such that short HRT may lead to VFA accumulation (Maaz et al. 2019). Thus, in this study, we found convenient to study with higher HRT than those reported DM-coupled UASB systems, which were mentioned above.

SS concentrations measured in the settling zone of the reactor and membrane effluent are presented in Fig. 6. At the beginning of the operational period, the initial SS concentration in the membrane effluent was 510 mg/L (Fig. 6b). The effluent solid concentration began to decrease owing to solid–liquid rejection on the support material. The effluent SS concentration then increased on day 31 with an increase in CFV and decreased to below 50 mg/L with the formation of an effective DM layer in the following days (Fig. 6b). The effluent SS concentration was maintained at a low level (48 ± 13 mg/L) throughout the stable operation phase. The operation ended with a SS concentration in the membrane effluent of 27 mg/L in this study. Alibardi et al. (2016) reported an effluent SS concentration of lower than 40 mg/L with a well-formed DM layer at the end of the operational period. Moreover, the effluent SS concentrations were comparable with those of other AnDMBR studies (Zhang et al. 2011; Yurtsever et al. 2021; Jiao et al. 2022). However, as mentioned by Alibardi et al. (2014), absolute SS removal could not be obtained by the AnDMBR in comparison with conventional membrane systems.

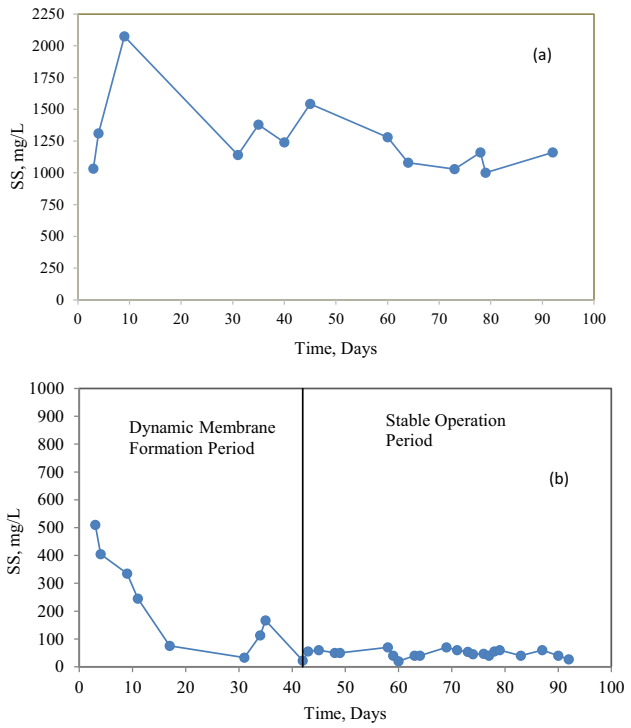

Fig. 6 SS in the settling zone of the reactor (**a**) and SS in the membrane effluent (**b**) during the AnDMBR operation

SS concentration in the settling of reactor was measured (1264 ± 289 mg/L) to detect the solid retainment by support material during the operational period (Fig. 6a). After DM formation, the DM-coupled UASB removed nearly 99% of SS. In addition, 96% of SS in the reactor was retained by well-formed DM. This showed that the DM could attain efficient solid rejections during high-strength wastewater treatment. Moreover, the attached SS over membrane was 213 g per support layer area. That was higher than Hu et al. (2018b). As mentioned before, increase in OLR can result more solid accumulation on support layer. It should be noted that the operation was done at a higher loading rate in this study compared to that reported study.

Studies have reported dairy wastewater treatment by conventional anaerobic processes. Sivakumar and Sekaran (2015) achieved 86% SS removal with an HRT of 5.21 d with a UASB reactor treating synthetic milk wastewater. The SRT and HRT in AnDMBRs become completely independent (Hu et al. 2018a). Therefore, a high sludge concentration can be obtained even with a short HRT (Liu et al. 2005). In this study, higher SS removal was obtained than those reported UASB studies.

The biogas production was 9.00 ± 2.90 L/d, and methane (CH_4) production was 5.03 ± 1.75 L/d with a CH_4 content of 57% (Fig. 7a). These values were higher than some reported studies. (Alibardi et al. 2016; Ersahin et al. 2017) owing to operation with a higher COD loading rate. The CH_4 yield in this study was in the range of 0.10–0.28 L CH_4/g $COD_{removed}$ (Fig. 7b). This was lower than the theoretical value. As mentioned by Ersahin et al. (2014), the actual amount of degraded COD converted to CH_4 was lower than the amount of COD removed. They indicated that up to 40–50% of the CH_4 could be solubilized in the membrane effluent. They also stated that there were some reported AnMBR studies that methane yield was in the range of 0.124–0.27 LCH_4/g$COD_{removed}$. The result of this study was consistent with this range. Moreover, the result in this study was higher than Yang et al. (2020), who reported a CH_4 yield in the range of 0.08 L–0.12 L CH_4/g $COD_{removed}$ during DM-coupled UASB reactor treatment. The VFA effluent concentration was approximately 500 mg/L, and acetic acid was the dominant acid in the beginning of the operational period (first 7 d of operation). The VFA concentration was mostly under detectable limits (< 10 mg/L), and isobutyric acid was detected in the remaining operational period. Owing to the retention of methanogenic microorganisms in the membrane system, VFA was mostly converted into CH_4.

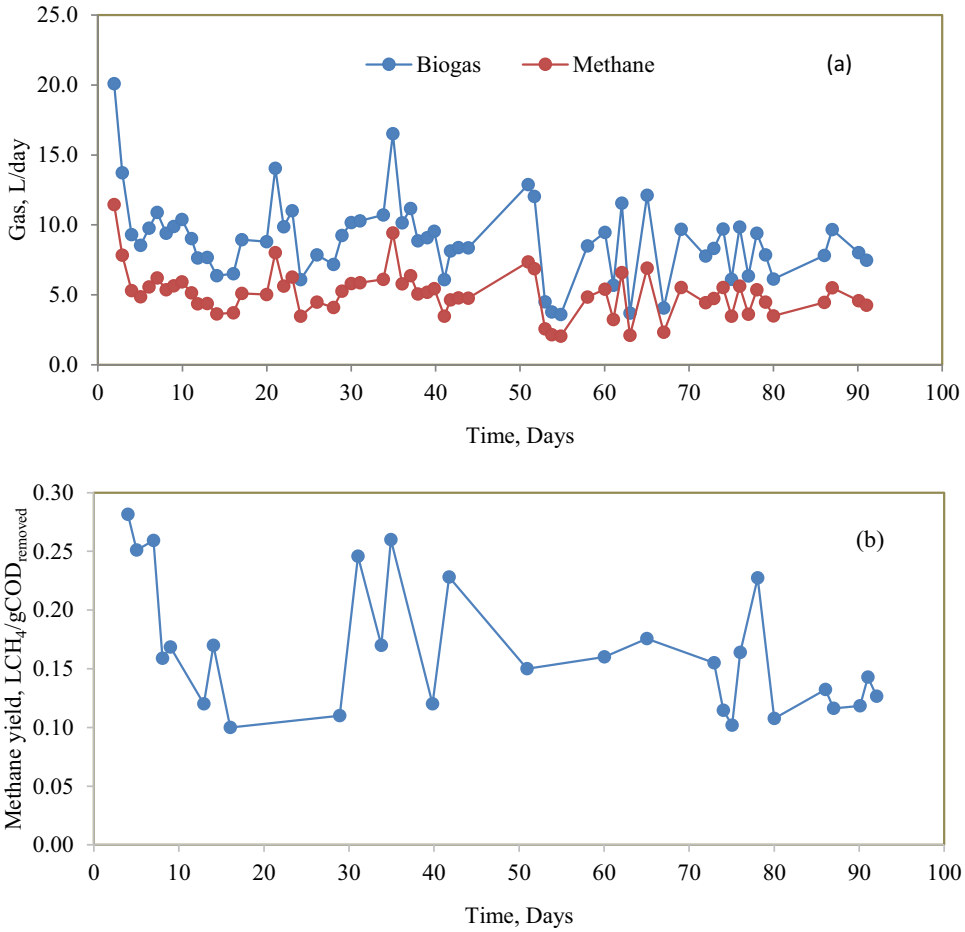

Fig. 7 Biogas and methane concentration (**a**) and methane yield (**b**) in the AnDMBR effluent

Morphological and chemical characteristics of the DM layer

PSD

The average particle sizes by volume were approximately 120 µm in the settling zone (Fig. 8a). These results showed that the sludge particles that had a size larger than the 20 µm pore size support material could easily accumulate on the DM layer and significantly decrease permeability of membrane. The support material of 20 µm pore size could result in rapid membrane fouling if the CFV and backwash were not applied. This showed the importance of cake layer control in long-term DM operation.

Moreover, the medium particle size of DM by volume was 700 µm pore size (Fig. 8b). As mentioned above, the average particle sizes by volume were 120 µm in the settling zone of the reactor; thus, particle size on the DM layer was higher than on settling zone. This result was consistent with Ersahin et al. (2016). This is because small particles could stick to each other since metal ions may act as a bridge between biopolymers, microbial cells, and they formed strict cake layer. As mentioned by Ersahin et al. (2016), the particle size may increase on support layer owing to this tight adherence.

SEM–EDX

Figure 9 presents the SEM micrograph of the virgin layer, gel layer, and DM. The surface of the virgin polyester nylon mesh, presented in Fig. 9a, demonstrates the smooth structure and porosity of the regularly oriented nylon mesh fibers. After the cake layer removed physically, it was observed that the residuals, which forming gel layer, adhered tightly to the support layer surface, such that C, Ca, P, and O deposited over the support material (Fig. 9b).

EDX analysis detected C, Ca, P, O, S elements in selected points of the DM layer (Fig. 9c). The inorganic elements were originated from the feed wastewater owing to acting as a source of trace elements for healthy growth of bacteria cells.

The cake layer is formed by interactions of divalent and trivalent cations (such as Ca^{+2}, Mg^{+2}, Fe^{+2}) with biopolymers. The organic foulants can catch metal ions via charge neutralization, and this enhances the formation of the cake layer (Meng et al. 2009). Organic substances and inorganic

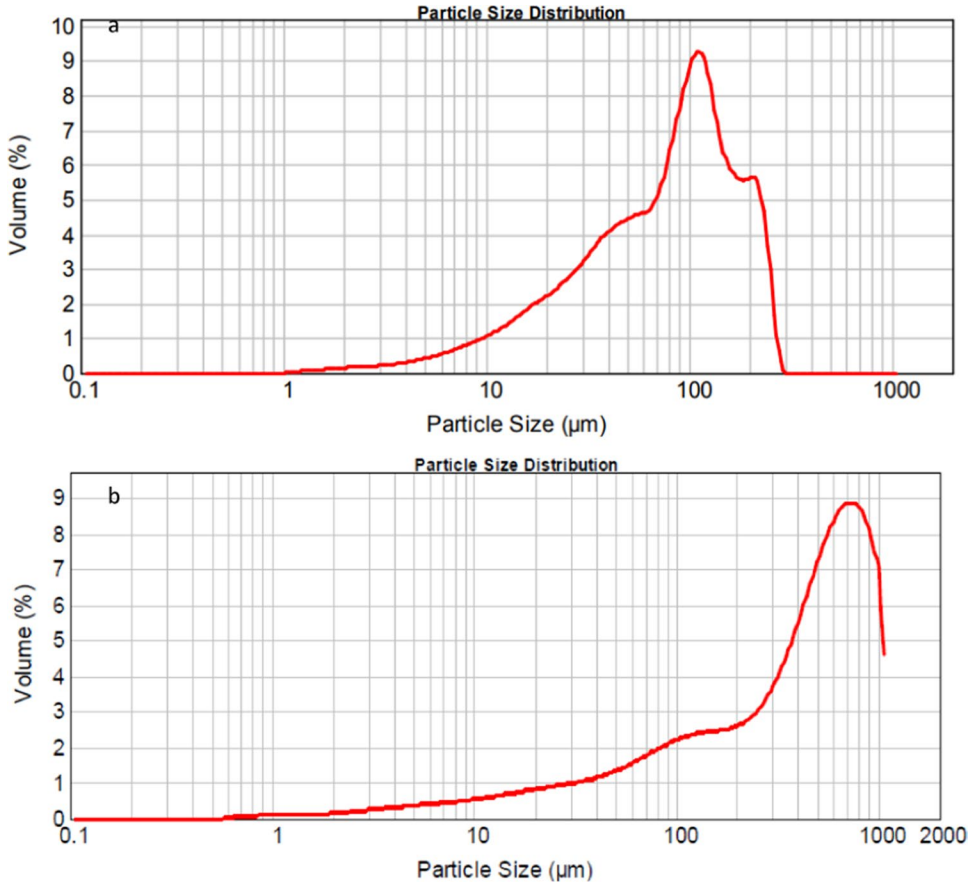

Fig. 8 PSD of the settling zone of the reactor (**a**) and DM layer (**b**)

elements were responsible for strict cake layer formation in this study. It should be noted that these other divalent and trivalent cations were detected by ICP-MS. The ionizable groups in cake layer such as carbonate ion (CO_3^{-2}), phosphate ion (PO_4^{-3}) and hydroxyl ion (^{-}OH) were detected by the FTIR analysis in this study. Meng et.al. (2009) reported that metal ions easily are taken possession by these negative ions, and this results in inorganic fouling. They added that because metal ions can also build bridge with biopolymers (e.g., carbohydrates, proteins), including ionizable groups (sulfate ion "SO_4^{-2}", PO_4^{-3}, carboxyl group "COO^{-}", CO_3^{-2}, OH^{-}) and the deposited cells, possessing negative charge under normal physiological conditions (Hulshoff et al. 2004). Thus, metal ions have an important role in the formation of fouling layers that results in formation of dense cake layer (Meng et al. 2009).

As mentioned above, these determined elements were mainly originated from the feed, so the type of substrate was significant for inorganic matter accumulation in the DM. As mentioned by Ersahin et al. (2016), the concentration of inorganic compounds in feed should be considered to handle DM control during the operation because these elements cause inorganic matter accumulation and improve cake layer formation.

FTIR

The peak at 3272.6 cm^{-1} demonstrated–OH stretching of polysaccharides (Fig. 10). The peak at 2920 cm^{-1} showed aliphatic C–H stretching (Smidt and Meissl 2007). The peak at 1629.5 cm^{-1} was in the region of 1700–1600 cm^{-1} in the spectrum, which is unique to the protein secondary structure of amides I (Alvarez et al. 2008). In addition, N–H wagging vibration at 711.6 cm^{-1} showed a secondary amide group (Smidt and Meissl 2007). The peak at 1415.5 cm^{-1} and the band in the range of 1200–1320 cm^{-1} represented the presence of amides III (C–N stretching and N–H bending). The broad peak at 1024 cm^{-1} and the band in the range of 1180–1260 cm^{-1} indicated that the C–O bonds were associated with polysaccharide or polysaccharide-like substances. The results of the FTIR spectrum showed the presence of polysaccharide-like substances and proteins in the cake layer (Ersahin et al. 2016). Extracellular polymeric substances (EPS) are biopolymers produced by deposited cells in a membrane (Meng et al. 2017) that consist mainly of polysaccharides, proteins, and deoxyribonucleic acid (DNA) (Costa et al. 2018). Considering all this information, as mentioned by Ersahin et al. (2016), the FTIR spectroscopy and SEM results demonstrated the presence of EPS.

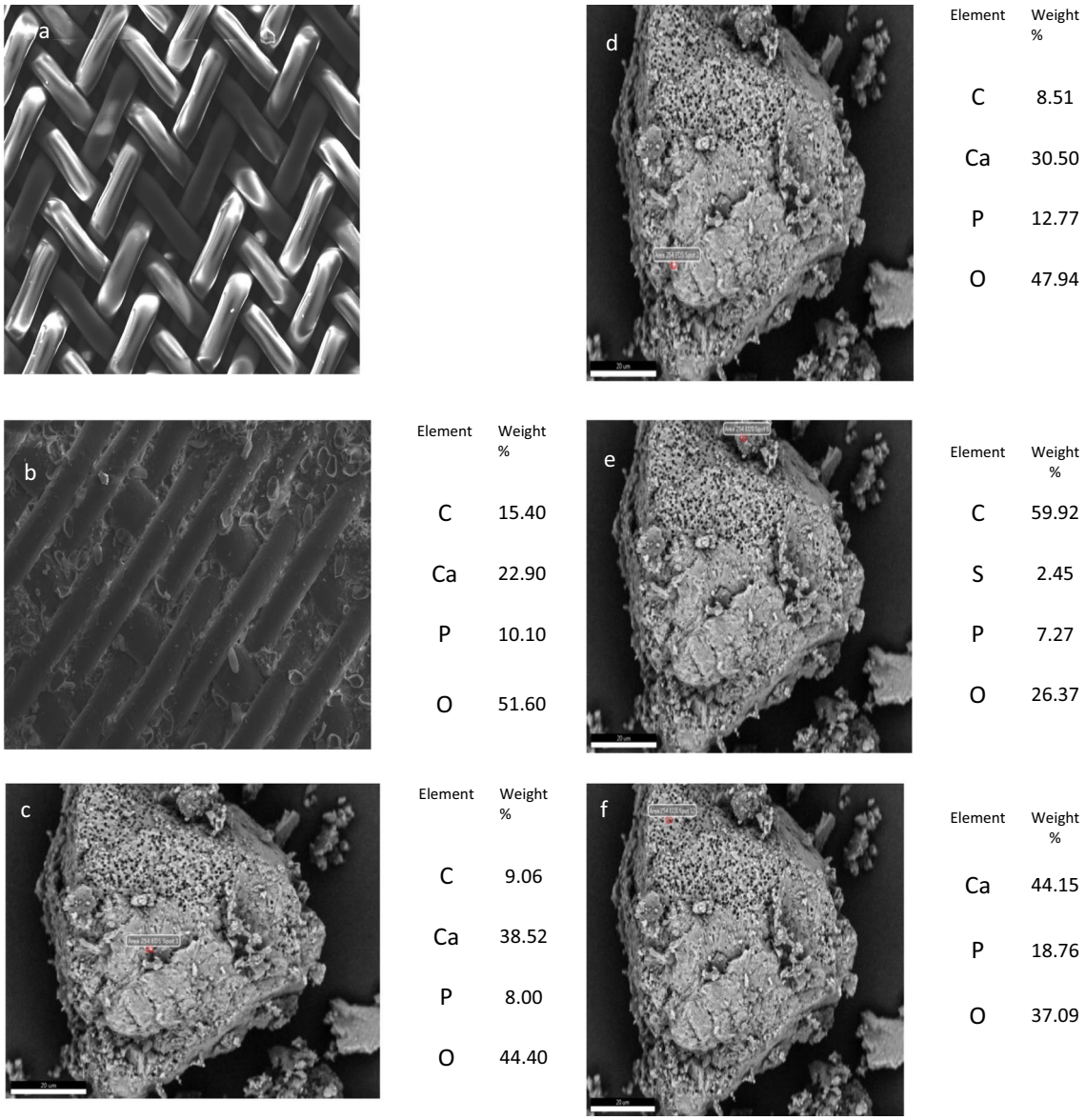

Fig. 9 SEM images: virgin support material (**a**), gel layer on support material (**b**) DM layer at the end of operation period (**c**, **d**, **e**, **f**)

Polysaccharides have properties such as large-size and gelation behavior. The gelling properties of polysaccharides strongly lead to their fouling tendency. The cross-linked chain in the polysaccharides creates the structure. Such that the gelling properties are commonly led by this structure. This gelation can be improved largely in the presence of divalent or multivalent cations due to the fact that these cations can play role as bridges for the carboxyl groups in polysaccharides. The presence of these cations can contribute to the formation of impermeable gels on membranes (Meng et al. 2017). In addition to this, the interactions between proteins and polysaccharides have high membrane fouling potential (Meng et al. 2017). Thus, this is one of reasons for the formation of dense cake layer in this study (Fig. 9c–f). The peak at 873.6 cm^{-1} represented the carbonate ion. This inferred that the degradation of feed into end-products (biogas) under anaerobic condition led to the release of inorganic ions such as Ca into solution and Ca reacted with carbonate ions and precipitated out (Marcato et al. 2008). Moreover, the sharp peak at 561.8 cm^{-1} was attributed to PO_4^{3-} groups (Mehdikhani and Borhani 2014). Ca^{2+} and PO_4^{3-} originated from milk. It could be inferred that the substrate type had a significant effect on the cake layer components. The peaks at 599.8, 491.8, 472.5, 459.0, and 451.3 cm^{-1} showed S–S stretching, originating from feed wastewater (Coates 2000). It can be inferred that the substrate type affected importantly the contents of cake layer.

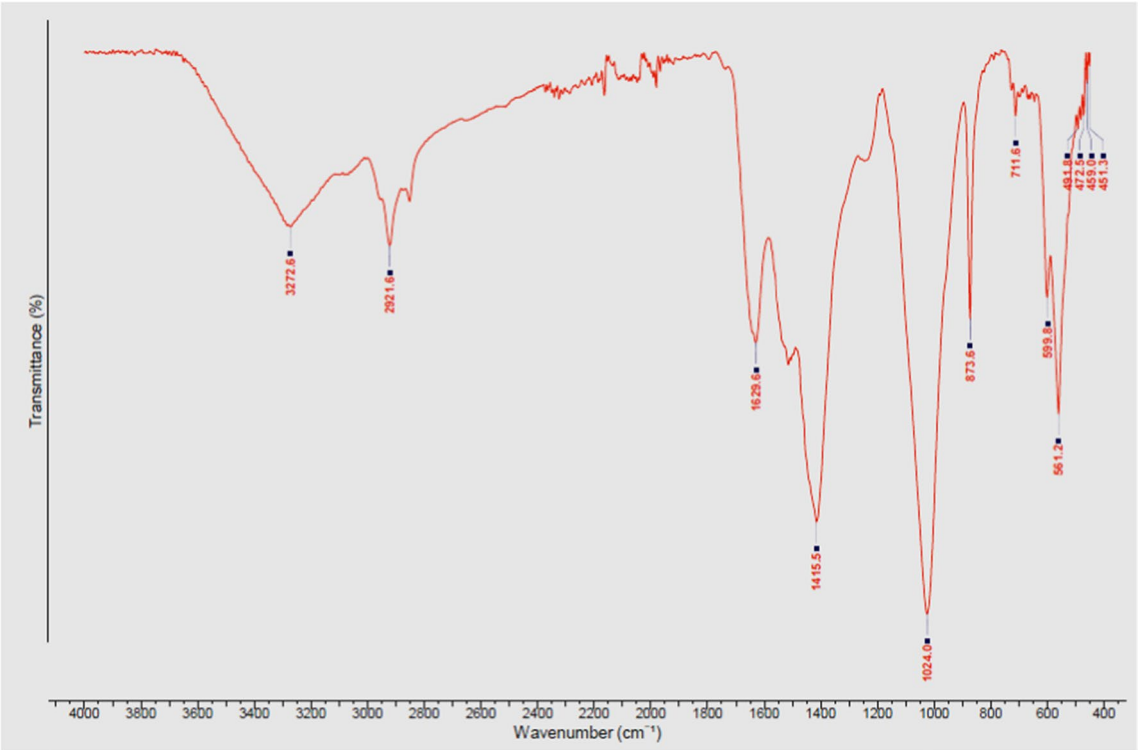

Fig. 10 FTIR spectrum of DM layer

ICP-MS

Metal ions play a very important role in dense cake layer formation because they make a connection between deposited cells and biopolymers (Meng et al. 2017). Thus, the heavy metal ions were investigated in the DM. ICP-MS detected 1.16 ± 0.08% Na, 1.50 ± 0.09% Mg, 0.76 ± 0.03% K, 3.34 ± 0.11% Ca, and 0.40 ± 0.01% Fe in mass concentration. Ersahin et al. (2016) detected similar elements in DM layer. As mentioned above, metal ions in the DM were responsible for the dense cake layer formation.

Conclusion

The AnDMBR increased organic matter removal by up to 99% with a COD loading rate of 8.1 ± 1.5 kg/(m^3 day). High COD removal was obtained by using a cheap nylon mesh in contrast to conventional membranes. This study showed that the application of CFV was a key factor in AnDMBR operation. The CFV and TMP applied in this study were lower than those of conventional membranes. This contributed to the low cost of the operation.

In addition, the DM application under anaerobic conditions not only obtained a high treatment efficiency, but also produced biogas, which makes it an attractive solution for both the treatment of high-strength wastewater and energy recovery. The analysis results showed that wastewater type had an important effect on well-formed cake layer. The metal ions, found in dairy wastewater, was one of important factor that responsible for dense cake layer. This study illustrated that a stable DM, which formed as a result of polysaccharides, and proteins, significantly improved organic matter removal.

Supplementary Information The online version contains supplementary material available at https://doi.org/10.1007/s13762-023-04767-2.

Acknowledgements The authors gratefully acknowledge for the financial support from The Scientific and Technological Research Council of Turkey (TUBITAK) (114Y812) and The Scientific Research Project Unit (FEN-C-DRP-120417-0182) in Marmara University.

Declarations

Conflict of interest The authors declare no conflict of interest

References

Alibardi L, Cossu R, Saleem M, Spagni A (2014) Development and permeability of a DM for anaerobic wastewater treatment. Bioresour Technol 161:236–244. https://doi.org/10.1016/j.biortech.2014.03.045

Alibardi L, Bernava N, Cossu R, Spagni A (2016) Anaerobic dynamic membrane bioreactor for wastewater treatment at ambient temperature. Chem Eng J 284:130–138. https://doi.org/10.1016/j.cej.2015.08.111

Alvarez PA, Ramasway HS, İsmail AA (2008) High pressure gelation of soyproteins: effect of concentration, pH and additives. J Food Eng 88:331–340. https://doi.org/10.1016/j.jfoodeng.2008.02.018

APHA (2005) Standard methods for the examination of water and waste-water. American Public Health Association/American Water Works Association/Water Environment Federation, Washington DC

Bangsbo-Hansen DI (1985) Treatment of dairy wastewater in the developing countries: the Danish experience. Ind Environ 8(4):10–12

Britz TJ, Van Schalkwyk C, Hung Y (2006) Treatment of dairy processing wastewaters. Taylor and Francis Group 1–28. https://ediscIplinas.usp.br

Chang I-S, Le-Clech P, Jefferson B, Judd S (2002) Membrane fouling in membrane bioreactors for wastewater. J Environ Eng 128(11):1018–1029. https://doi.org/10.1061/(ASCE)0733-9372(2002)128:11(1018)

Coates J (2000) Interpretation of infrared spectra, a practical approach. In: Meyers RA (ed) Encyclopedia of analytical chemistry. Wiley, Chichester, pp 10815–10837

Costa OY, Roaijmakers JM, Kuramae EE (2018) Microbial extracellular polymericsubstances: ecological function and impact on soil aggregation. Front Microbiol 9:1–14. https://doi.org/10.3389/fmicb.2018.01636

Couras CS, Louros VL, Gamerio NA, Silva A, Capela MI, Arroa LM, Nadais H (2015) Anaerobic degradation of dairy wastewater in intermittent UASB reactors:influence of effluent recirculation. Environ Technol 36(17):2227–2238. https://doi.org/10.1080/09593330.2015.1025102

Daud MK, Rizvi H, Akram MF, Ali S, Rizwan M, Nafees M, Jin ZS (2018) Review of upflow anaerobic sludge blanket reactor technology: effect of different parameters and developments for domestic wastewater treatment. J Chem 2018:1–13. https://doi.org/10.1155/2018/1596319

Dereli RK, van der Zee FP, Ozturk İ, van Lier JB (2019) Treatment of cheese whey by a cross-flow anaerobic membrane bioreactor: biological and filtration performance. Environ Res 168:109–117. https://doi.org/10.1016/j.envres.2018.09.021

Du X, Shi Y, Jegatheesan V, Hoq IU (2020) A review on the mechanism, impacts and control methods of membrane fouling in MBR system. Membrane 10(2):24. https://doi.org/10.3390/membranes10020024

Elangovan C, Sekar A (2012) Application of up flow anaerobic sludge blanket (UASB) reactor process for the treatment of dairy wastewater: a review. Nat Environ Pollut Technol 11:409–414

Ersahin ME, Ozgun H, Dereli RK, Ozturk I, Roest K, van Lier JB (2012) A review on dynamic membrane filtration: materials, applications and future perspectives. Bioresour Technol 122:196–206. https://doi.org/10.1016/j.biortech.2012.03.086

Ersahin ME, Ozgun H, Tao Y, van Lier JB (2014) Applicability of DM technology in anaerobic membrane bioreactors. Water Resour 48:420–429. https://doi.org/10.1016/j.watres.2013.09.054

Ersahin ME, Tao Y, Ozgun H, Spanjers H, van Lier JB (2016) Characteristics and role of dynamic membrane layer in anaerobic membrane bioreactors. Biotechnol Bioeng 113(4):761–771. https://doi.org/10.1002/bit.25841

Ersahin ME, Tao Y, Ozgun H, Gimenez JB, Spanjers H, van Lier JB (2017) Impact of anaerobic dynamic membrane bioreactor configuration on treatment and filterability performance. J Membr Sci 526:387–394. https://doi.org/10.1016/j.memsci.2016.12.057

Forero FL, Vélez PC, Sandoval AP (2013) Ultrafiltration and osmotic evaporation applied to the concentration of cholupa (*Passiflora maliformis*) juice. Ingenieria E Investigacion 33(1):35–40

Giordani A, Brucha G, Santos KA, Rojas K, Hoyoski E, Alves MMS, Tommaso G (2021) Performance and microbial community analysis in an anaerobic hydrid baffled reactor treating dairy wastewater. Water Air Soil Pollut 232(10):1–16. https://doi.org/10.1007/s11270-021-05348-0

Hu Y, Wang CX, Ngo HH, Sun Q, Yang Y (2018a) Anaerobic DM bioreactor (AnDMBR) for wastewater treatment: a review. Bioresour Technol 247:1107–1118. https://doi.org/10.1016/j.biortech.2017.09.101

Hu Y, Yang Y, Yu S, Wang X, Tang J (2018b) Psychrophilic anaerobic dynamic membrane bioreactor for domestic wastewater treatment: effects of organic loading and sludge recycling. Bioresour Technol 270:62–69. https://doi.org/10.1016/j.biortech.2018.08.128

Hulshoff LW, de Castro Lopes SI, Lettinga G, Lens PNL (2004) Anaerobic sludge granulation. Water Resource 38:1376–1389. https://doi.org/10.1016/j.watres.2003.12.002

Jeison D, van Lier JB (2007) Cake formation and consolidation main factors governing the applicable flux in anaerobic submerged membrane reactors (AnSMBR) treating acidified wastewaters. Sep Purif Technol 56:71–78. https://doi.org/10.1016/j.seppur.2007.01.022

Jiao C, Hu Y, Zhang X, Jing R, Zeng T, Chen R, Li Y (2022) Process characteristics and energy self-sufficient operation of a low-fouling anaerobic dynamic membrane bioreactor for up-concentrated municipal wastewater treatment. Sci Total Environ 843:156992

Joshiba GJ, Kumar PS, Femina CC, Jayashree E, Racchara R, Sivanesan S (2019) Critical review on biological treatment strategies of dairy wastewater. Desalin Water Treat 160:94–109. https://doi.org/10.5004/dwt.2019.24194

Judd S (2006) The MBR Book: Principles and application of membrane bioreactors in water and wastewater treatment, 1st edn. Elsevier, Amsterdam, Holland

Karadağ D, Köroğlu OE, Ozkaya B, Cakmakcı M, Heaven S, Banks C, Sema-Maza A (2015a) Anaerobic granular reactors for the treatment of dairy wastewater: a review. Int J Dairy Technol 68(4):459–470. https://doi.org/10.1111/1471-0307.12252

Karadağ D, Köroğlu OE, Ozkaya B, Cakmakcı M (2015b) A review on anaerobic biofilm reactors for the treatment of dairy industry wastewater. Process Biochem 50:262–271. https://doi.org/10.1016/j.procbio.2014.11.005

Karthiyen K, Kandasamy J (2009) Upflow anaerobic sludge blanket (UASB) reactor in wastewater treatment. Water Wastewater Treat Technol 2:180–198

Kooijman G, Lopes W, Zhou Z, Guo H, de Kreuk M, Spanjers H, van Lier J (2017) Impact of coagulant and flocculant addition to an anaerobic dynamic membrane bioreactor (AnDMBR) treating waste-activated sludge. Membranes 7(2):18. https://doi.org/10.3390/membranes7020018

Le Clech P, Jefferson B, Chang IS, Judd SJ (2003) Critical flux determination by the flux-step method in a submerged membrane bioreactor. J Membr Sci 227:81–93. https://doi.org/10.1016/j.memsci.2003.07.021

Li L, Xu G, Yu H (2017) Dynamic membrane filtration: formation, filtration, cleaning and applications. Chem Eng Technol 41(1):7–18. https://doi.org/10.1002/ceat.201700095

Lin HJ, Xie K, Mahendran B, Bagley DM, Leung KT, Liss SN, Liao BQ (2009) Sludge properties and their effects on membrane fouling in submerged anaerobic membrane bioreactors (SAnMBRs). Water Res 43(15):3827–3837. https://doi.org/10.1016/j.watres.2009.05.025

Lin H, Peng W, Zhang M, Chen J, Hong H, Zhang Y (2013) A review on anaerobic membrane bioreactors: applications, membrane fouling and future perspectives. Desalination 314:169–188. https://doi.org/10.1016/j.desal.2013.01.019

Liu R, Huang X, Chen L, Wen X, Qian Y (2005) Operational performance of a submerged membrane bioreactor for reclamation of

bath wastewater. Process Biochem 40(1):125–130. https://doi.org/10.1016/j.procbio.2003.11.038
Maaz M, Yasin M, Aslam M, Kumar G, Atabari AE, Idrees M, Anjum F, Jamil F, Ahmad R, Khan AL, Lesage G, Heran M, Kim J (2019) Anaerobic membrane bioreactors for wastewater treatment: configurations, fouling control and energy considerations. Bioresour Technol 283:358–372. https://doi.org/10.1016/j.biortech.2019.03.061
Mahat SM, Omar R, Idris A, Kamal S, Idris A (2018) Dynamic membrane applications in anaerobic and aerobic digestion for industrial wastewater: a mini review. Food Bioprod Process 112:150–168. https://doi.org/10.1016/j.fbp.2018.09.008
Marcato CE, Mohtar R, Revel JC, Poliech P, Hafidi M, Guirresse M (2008) Impact of anaerobic digestion on organic matter quality in pig slurry. Int Biodeterior Biodegradation 63:260–266. https://doi.org/10.1016/j.ibiod.2008.10.001
Mehdikhani B, Borhani GH (2014) Densification and mechanical behavior of β-tricalcium phosphate bioceramics. Int Lett Chem 36:37–49
Meng F, Chae SR, Drews A, Kramue M, Shin HS, Yang F (2009) Recent advances in membrane bioreactors (MBRs): membrane fouling and membrane material. Water Resour 43:1489–1512. https://doi.org/10.1016/j.watres.2008.12.044
Meng F, Zhang S, Oh Y, Zhou Z, Shin HS, Chae SR (2017) Fouling in membrane bioreactors: an updated review. Water Resour 114:151–180. https://doi.org/10.1016/j.watres.2017.02.006
Pacal M, Semerci N, Çallı B (2019) Treatment of synthetic wastewater and cheese whey by the anaerobic DM bioreactor. Environ Sci Pollut Res 26:32942–32956. https://doi.org/10.1007/s11356-019-06397-z
Quek PJ, Yeap TS, Ng HY (2017) Applicability of upflow anaerobic sludge blanket and DM-coupled process for the treatment of municipal wastewater. Appl Microbiol Biotechnol 101:6531–6540
Ramon GZ, Hoek EMV (2012) On the enhanced drag force induced by permeation through a filtration membrane. J Membr Sci 392–393:1–8. https://doi.org/10.1016/j.memsci.2011.10.056
Satyawali Y, Balakrishnan M (2008) Treatment of distillery effluent in a membranebioreactor (MBR) equipped with mesh filter. Sep Purif Technol 63(2):278–286. https://doi.org/10.1016/j.seppur.2008.05.008
Siddiqui MA, Biswal BK, Saleem M, Guan D, Iqbal A, Wu D, Khanal SK, Chen G (2021) Anaerobic self-forming dynamic membrane bioreactors (AnSFDMBRs) for wastewater treatment: recent advances, process optimization and perspectives. Bioresour Technol 332:125101. https://doi.org/10.1016/j.biortech.2021.125101
Siddiqui MA, Heynderickx D, Khanal SK, Chen GH, Wu D (2022) Dynamic anaerobic membrane bioreactor coupled with sulfate reduction (SrDMBR) for saline wastewater treatment. Bioresour Technol 346:126447. https://doi.org/10.1016/j.biortech.2021.126447
Sivakumar R, Sekaran V (2015) Comparative study of performance evaluation of UASB reactor for treating synthetic dairy effluent at psychrophilic and mesophilic temperatures. Nat Environ Pollut Technol 14(3):679–684
Slavov A (2017) General characteristics and treatment possibilities of dairy wastewater: a review. Food Technol Biotechnol 55(1):14–28
Smidt E, Meissl K (2007) The applicability of Fourier transform infrared (FT-IR) spectroscopy in waste management. Water Manag 27(2):268–276. https://doi.org/10.1016/j.wasman.2006.01.016
Sun F, Zhang N, Li F, Wang X, Zhang J, Song L, Liang S (2018) Dynamic analysis of self-forming DM(SFDM) filtration in submerged anaerobic bioreactor: performance, characteristic, and mechanism. Bioresour Technol 270:383–390. https://doi.org/10.1016/j.biortech.2018.09.003
Tan LC, Peschard R, Deng Z, Ferreira ALM, Lens PNL, Pacheco-Ruiz S (2021) Anaerobic digestion of dairy wastewater by side-stream membrane bioreactors: comparison of feeding regime and its impact on sludge filterability. Environ Technol Innov 22:101482. https://doi.org/10.1016/j.eti.2021.101482
Tang J, Wang XC, Hu Y, Ngo HH, Li Y (2017) DM-assisted fermentation of food wastes for enhancing lactic acid production. Bioresour Technol 234:40–47. https://doi.org/10.1016/j.biortech.2017.03.019
Wang J, Cahyali A, Wu B, Pee W, Fane AG, Chew JW (2020) The roles of particles in enhancing membrane filtration: a review. J Membr Sci 595:117570. https://doi.org/10.1016/j.memsci.2019.117570
Yang Y, Hu Y, Wang X, Ngo H (2020) Up-flow anaerobic dynamic membrane bioreactor (AnDMBR) for wastewater treatment at room temperature and short hrts: process characteristics and practical applicability. Chem Eng J 383:123–186. https://doi.org/10.1016/j.cej.2019.123186
Yurtsever A, Basaran E, Ucar D, Sahinkaya E (2021) Self-forming dynamic membrane bioreactor for textile industry wastewater treatment. Sci Total Environ 751:141572. https://doi.org/10.1016/j.scitotenv.2020.141572
Zhang X, Wang Z, Wu Z, Wei T, Lu F, Tong J, Mai S (2011) Membrane fouling in an anaerobic dynamic membrane bioreactor (AnDMBR) for municipal wastewater treatment: characteristics of membrane foulants and bulk sludge. Process Biochem 46(8):1538–1544. https://doi.org/10.1016/j.procbio.2011.04.002
Zhang Y, Zhao Y, Chu H, Dong B, Zhou X (2014) Characteristics of dynamic membrane filtration: structure, operation mechanisms, and cost analysis. Sci Bull 59(3):247–260. https://doi.org/10.1007/s11434-013-0048-x